Inorganic Chemistry
Article

Inorg. Chem. **2010**, *49*, 10635–10641 **10635**
DOI: 10.1021/ic1016438

Harnessing Low-Valent Metal Centers through Non-Bonding Orbital Interactions

Titel Jurca,[†] Ilia Korobkov,[†] Glenn P. A. Yap,[‡] Serge I. Gorelsky,*[,†] and Darrin S. Richeson*[,†]

[†]*Centre for Catalysis Research and Innovation and Department of Chemistry, University of Ottawa, Ottawa, Ontario K1N 6N5, Canada, and* [‡]*Department of Chemistry and Biochemistry, University of Delaware, Newark, Delaware 19716, United States*

Received August 12, 2010

The synthesis, characterization, and computational analysis of a series of low-valent, In(I) complexes bearing the bis(imino)pyridine scaffold, $\{Ar'N{=}CPh\}_2(NC_5H_3)$, is reported. A stepwise steric reduction of the aryl groups on the imine substituents around the coordination site, (Ar′ = 2,5-^{t}Bu$_2$C$_6$H$_3$, 2,6-^{i}Pr$_2$C$_6$H$_3$, 2,6-$(CH_3CH_2)_2C_6H_3$) is explored through the spectroscopic and crystallographic examination of complexes $[\{Ar'N{=}CPh\}_2(NC_5H_3)]In^+(OTf)^-$ (**1**−**3**). Compounds **1**−**3** displayed long In−N and In−OTf distances indicating only weak or no coordination. Application of the ligand with Ar′ = 2,6-$(CH_3)_2C_6H_3$ led to an In(III) bis(imino)pyridine complex, $[\{2,6\text{-}Me_2C_6H_3N{=}CPh\}_2(NC_5H_3)]In(OTf)_2Cl$ **4** with coordinated ligand, chloride, and triflate groups. Computational analysis of the interactions between the In cation and the ligands (orbital populations, bond order, and energy decomposition analysis) point to only minimal covalent interactions of the In(I) cation with the ligands. Although it features three N donor centers, the bis(imino)pyridine ligand provides little ligand-to-metal donation. A thorough electronic structure analysis revealed a correlation of compound stability with the reduced contribution of the In(I) 5s lone electron pair to the highest occupied molecular orbital (HOMO) of the cation. This effect, originating from non-bonding orbital interactions between the metal and the ligand, is more prominent in sterically crowded environments. The discovery of this correlation may help in designing new low-valent complexes.

Introduction

Challenges to conventional metal−ligand bonding interactions are presented by the recent crystallographic characterization and computational scrutinization of reactive species that display only nominal classic Lewis acid/base coordination.[1,2] These efforts raise fundamental bonding questions that in turn inspire the synthesis of increasingly challenging target molecules. The judicious choice of metal cation environment/ligand array appears to play an essential role in these issues. In the case of indium(I), the exceptionally sterically encumbering ortho-terphenyl ligand, 2,6-$(Tripp)_2C_6H_3$ (Tripp = 2,4,6-^{i}Pr$_3$C$_6$H$_2$), allowed the isolation of the unique example of single-coordination of this metal cation as 2,6-$(Tripp)_2C_6H_3In(I)$.[3] Slightly reducing the bulk of the ligand to 2,6-$(Dipp)_2C_6H_3$ (Dipp = 2,6-^{i}Pr$_2$C$_6$H$_3$), yielded a "diindene" dimer $[2,6\text{-}(Dipp)_2C_6H_3In]_2$ with an In−In bond.[4] The isolation of a cryptand encapsulated Ge cation, $(Ge\ cryptand[2.2.2])^{2+}(O_3SCF_3)^-{}_2$, revealed a species with the dicationic group 14 element possessing a lone pair of electrons, three unoccupied valence orbitals, and no tightly covalently bonded ligands. This unique metalloid complex apparently possessed insubstantial Ge−N and Ge−O bonding interactions. These efforts have recently expanded to demonstrate that azamacrocycles and crown ethers are suitable ligands for isolation of germanium dication species.[5,6] Our recent isolation and characterization of $[\{2,5\text{-}^tBu_2C_6H_3N{=}CPh\}_2(NC_5H_3)]In^+(OTf)^-$ **1**, bearing a sterically demanding bis(imino)pyridine ligand, presented a species with a single long In−N(pyridine) interaction and an electronic structure for the cation indicating that the In^+ ion accepts little covalent donor−acceptor interactions from the ligand.

Our elaboration of these initial investigations is reported herein. The modular steric features of the bis(imino)pyridine scaffold are exploited with the synthesis of a systematic series of these ligands displaying varying steric load. Application of these ligands to the synthesis of a family of In complexes revealed a correlation of stability of these In(I) species with

*To whom correspondence should be addressed. E-mail: darrin@uottawa.ca (D.S.R.).

(1) Rupar, P. A.; Staroverov, V. N.; Baines, K. M. *Science* **2008**, *322*, 1360.
(2) Jurca, T.; Lummis, J.; Burchell, T. J.; Gorlesky, S. I.; Richeson, D. S. *J. Am. Chem. Soc.* **2009**, *131*, 4608.
(3) Haubrich, S. T.; Power, P. P. *J. Am. Chem. Soc.* **1998**, *120*, 2202.
(4) Wright, R. J.; Phillips, A. D.; Hardman, N. J.; Power, P. P. *J. Am. Chem. Soc.* **2002**, *124*, 8538.
(5) Cheng, F.; Hector, A. L.; Levason, W.; Reid, G.; Webster, M.; Zhang, W. *Angew. Chem., Int. Ed.* **2009**, *48*, 5152. Rupar, P. A.; Bandyopadhyay, R.; Cooper, B. F. T.; Stinchcombe, M. R.; Ragogna, P. J.; Macdonald, C. L. B.; Baines, K. M. *Angew. Chem., Int. Ed.* **2009**, *48*, 5155.
(6) Crown ether complexes of In(I)-OTf are reported in (a) Andrews, C. G.; Macdonald, C. L. B. *Angew. Chem., Int. Ed.* **2005**, *44*, 7453. (b) Cooper, B. F. T; Macdonald, C. L. B. *J. Organomet. Chem.* **2008**, *693*, 1707.

Published on Web 10/12/2010

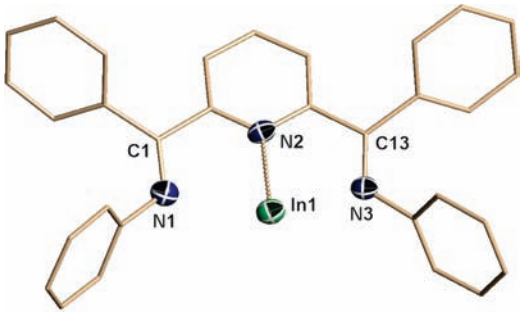

Figure 1. X-ray structure of the $[\{2,5\text{-}^{t}Bu_2C_6H_3N{=}C(Me)\}_2(NC_5H_3)]In^{+}$ cation of compound **1**. Hydrogen atoms, *tert*-butyl groups, and triflate counterion have been omitted for clarity.

Scheme 1. Bis(imino)pyridine Ligands Used in This Report

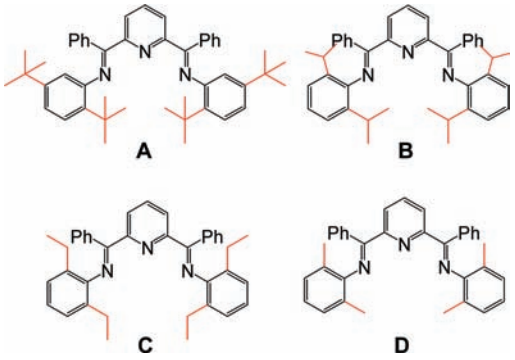

Scheme 2

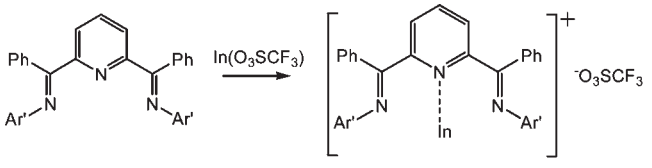

Ar'=2,5-$^{t}Bu_2C_6H_3$ **1**; 2,6-$^{i}Pr_2C_6H_3$ **2**; 2,6-$Et_2C_6H_3$ **3**

the complexity and steric demand of the ligand substituents. Our thorough computational assessment of these compounds expands on the concept that sterically encumbered ligands can provide kinetic stabilization to reactive species with only weak coordination and electron donation.

Results and Discussion

The first low-valent, main group metal complex of the bis(imino)pyridine scaffold was recently prepared when the soluble and readily accessible In(I) synthon, $In(O_3SCF_3)$,[7] was allowed to react with ligand **A** (Schemes 1 and 2) to provide an excellent isolated yield (76%) of the bright orange compound **1**.[2] The bulky steric environment provided by the 2,5-$^{t}Bu_2C_6H_3$ substituents of the imine function in **A** were a key feature of the observed species. The identity of this species as the bis(imino)pyridine complex $[\{2,5\text{-}^{t}Bu_2C_6H_3N{=}CPh\}_2(NC_5H_3)]\text{-}In^{+}(OTf)^{-}$ **1** was established by single crystal X-ray analysis, and the results for the cationic component are summarized in Figure 1 and Tables 1 and 2.

Through a combined structural investigation and density-functional theory (DFT) analysis, In(I) complex **1** was revealed to display minimal metal−ligand coordination. Notably, **1** is monomeric with a long In−N2 bond distance of 2.495(5) Å.[8,9] The most direct comparisons to **1** can be made with In(I) complexes of anionic ligands. For example, the In−N bond distance in the two coordinate β-diketiminate complex $[In\{(NDippCMe)_2CH\}]$ is 2.27 Å.[10] Furthermore, for the three coordinate tris(3,5-di-*tert*-butylpyrazolyl)hydroborato In(I) these distances averaged about 2.47 Å[11] and for the four coordinate amidinato species [DippNC(tBu)NDipp]In(I) an In−N distance of 2.329(5) Å was observed.[12] The In center in **1** lies slightly out of the mean plane defined by the three N centers of the ligand (26.1°). The $In-N_{imine}$ distances, In−N1 2.747(5) Å and In−N3 2.689(5) Å, are beyond the sum of the covalent radii for In and N (covalent radius N = 0.71 Å, In = 1.42 Å).[13]

Furthermore, the long In−O(triflate) distance (In−O2 7.975 Å) was consistent with no or very little coordination of the anion.[6,7] The shortest In/triflate contact observed for **1** is to an F atom of the CF_3 group at a distance of 6.485 Å. Within **1**, the imine C=N distances (N1−C1 1.281(9) Å, N3−C13 1.283(9) Å) are comparable to those for the free ligand, and the carbon centers of the imine moieties are planar.[2] The SO bonds within the triflate anion are essentially equivalent and range from 1.406(7) Å to 1.425(6) Å. These values are consistent with a non-coordinated anion. All of these structural features point to the fact that **1** displayed a very weakly coordinated In center in spite of the presence of additional sites for coordination. Interestingly, the structural features for the singly coordinated cation **1** are reminiscent of the In(terphenyl) monomer 2,6-$(Tripp)_2C_6H_3In$.[3]

The periphery of the bis(imino)pyridine ligand **A** can be readily modified to provide a systematic reduction in steric bulk via stepwise removal of CH_3 groups from the $N_{imine}-Ar'$ substituents. The new bis(imino)pyridines, **B**−**D**, were prepared using a modified literature synthesis.[2,14] The modular steric features and the relative ease of synthesis for these species, along with the fact that the application of this ligand framework in main group chemistry is underdeveloped,[15,16] further inspired our efforts.

Like **A**, ligands **B** and **C** also react smoothly with $In(OSO_2CF_3)$, to provide orange compounds **2** and **3** in isolated

(7) Macdonald, C. L. B.; Corrente, A. M.; Andrews, C. G.; Taylor, A.; Ellis, B. D. *Chem. Commun.* **2004**, 250.

(8) For reviews of low valent In chemistry see: (a) Pardoe, J. A. J.; Downs, A. *J. Chem. Rev.* **2007**, *107*, 2. (b) Schmidbaur, H. *Angew. Chem., Int. Ed. Engl.* **1985**, *24*, 893.

(9) This distance is similar to that in the metastable complex InBr·TMEDA. Green, S. P.; Jones, C.; Stasch, A. *Chem. Commun.* **2008**, 6285.

(10) Hill, M. S.; Hitchcock, P. B. *Chem Commun.* **2004**, 1818.

(11) Kuchta, M. C.; Dias, H. V. R.; Bott, S. G.; Parkin, G. *Inorg. Chem.* **1996**, *35*, 943.

(12) Jones, C.; Junk, P. C.; Platts, J. A.; Rathmann, D.; Stasch, A. *Dalton Trans.* **2005**, 2497.

(13) Cordero, B.; Gómez, V.; Platero-Prats, A. E.; Revés, M.; Echeverría, J.; Cremades, E.; Barragán, F.; Alvarez, S. *Dalton Trans.* **2008**, 2832.

(14) Kleigrewe, N.; Steffen, W.; Blömker, T.; Kehr, G.; Fröhlich, R.; Wibbeling, B.; Erker, G.; Wasilke, J.-C.; Wu, G.; Bazan, G. C. *J. Am. Chem. Soc.* **2005**, *127*, 13955.

(15) For examples of main group bis(imino)pyridine compounds see: (a) Martin, C. D.; Le, C. M.; Ragogna, P. J. *J. Am. Chem. Soc.* **2009**, *131*, 15126. (b) Reeske, G.; Cowley, A. H. *Chem. Commun.* **2006**, 1784. (c) Reeske, G.; Cowley, A. H. *Chem. Commun.* **2006**, 4856. (d) Knijnenburg, Q.; Smits, J. M. M.; Budzelaar, P. H. M. *Organometallics* **2006**, *25*, 1036. (e) Blackmore, I. J.; Gibson, V. C.; Hitchcock, P. B.; Rees, C. W.; Williams, D. J.; White, A. J. P. *J. Am. Chem. Soc.* **2005**, *127*, 6012. (f) Scott, J.; Gambarotta, S.; Korobkov, I.; Knijnenburg, Q.; de Bruin, B.; Budzelaar, P. H. M. *J. Am. Chem. Soc.* **2005**, *127*, 17204. (g) Bruce, M.; Gibson, V. C.; Redshaw, C.; Solan, G. A.; White, A. J. P.; Williams, D. J. *Chem. Commun.* **1998**, 2523. (h) Baker, R. J.; Jones, C.; Kloth, M.; Mills, D. P. *New J. Chem.* **2004**, *28*, 2017. (i) Knijnenburg, Q.; Smits, J. M. M.; Budzelaar, P. H. M. *C. R. Chim.* **2004**, *7*, 865.

(16) Abram, S.; Maichle-Mössmer, C.; Abram, U. *Polyhedron* **1997**, *16*, 2183.

Table 1. Selected Bond Distances for Compounds **1**−**3** (Å)

1		**2**		**3**	
C(1)−C(8)	1.500(10)	C(13)−C(20)	1.502(9)	C(7)−C(8)	1.496(12)
C(12)−C(13)	1.488(10)	C(24)−C(25)	1.495(9)	C(12)−C(13)	1.497(12)
In(1)−N(2)	2.495(5)	In(1)−N(2)	2.502(5)	In(1)−N(2)	2.501(8)
In(1)−N(1)	2.747(5)	In(1)−N(1)	2.664(5)	In(1)−N(1)	2.731(8)
In(1)−N(3)	2.689(5)	In(1)−N(3)	2.679(5)	In(1)−N(3)	2.637(6)
In(1)−O(2)	7.975	In(1)−O(1)	2.462(6)	In(1)−O(1)	2.532(7)
N(1)−C(1)	1.281(9)	N(1)−C(13)	1.272(8)	N(1)−C(7)	1.268(11)
N(3)−C(13)	1.283(9)	N(3)−C(25)	1.272(8)	N(3)−C(13)	1.280(12)
N(2)−C(8)	1.329(9)	N(2)−C(20)	1.337(8)	N(2)−C(8)	1.368(11)
N(2)−C(12)	1.340(9)	N(2)−C(24)	1.350(8)	N(2)−C(12)	1.357(10)
N(1)−C(20)	1.426(9)	N(1)−C(6)	1.437(8)	N(1)−C(20)	1.433(11)
N(3)−C(34)	1.432(9)	N(3)−C(37)	1.446(8)	N(3)−C(30)	1.461(12)
O(1)−S(1)	1.425(6)	O(1)−S(1)	1.462(6)	O(1)−S(1)	1.460(7)
O(2)−S(1)	1.408(7)	O(2)−S(1)	1.421(7)	O(2)−S(1)	1.475(7)
O(3)−S(1)	1.419(8)	O(3)−S(1)	1.435(7)	O(3)−S(1)	1.418(8)

Table 2. Selected Bond Angles for Compounds **1**−**3** (deg)

1		**2**		**3**	
O(2)−In(1)−N(2)		O(1)−In(1)−N(2)	75.8(2)	O(1)−In(1)−N(2)	76.6(2)
In(1)−O(2)−S(1)		In(1)−O(1)−S(1)	138.0(4)	In(1)−O(1)−S(1)	178.3(5)
In(1)−N(2)−C(8)	121.0(4)	In(1)−N(2)−C(20)	120.7(4)	In(1)−N(2)−C(8)	122.0(6)
In(1)−N(2)−C(12)	118.8(4)	In(1)−N(2)−C(24)	120.6(4)	In(1)−N(2)−C(12)	119.3(6)
In(1)−N(1)−C(1)	109.71	In(1)−N(1)−C(13)	116.46	In(1)−N(1)−C(7)	116.65
In(1)−N(3)−C(13)	108.68	In(1)−N(3)−C(25)	115.89	In(1)−N(3)−C(13)	118.4(6)
N(1)−In(1)−N(2)	61.85	N(1)−In(1)−N(2)	63.62	N(1)−In(1)−N(2)	63.56
N(3)−In(1)−N(2)	63.09	N(3)−In(1)−N(2)	63.15	N(3)−In(1)−N(2)	64.7(2)
N(1)−C(1)−C(8)	116.1(6)	N(1)−C(13)−C(20)	118.5(6)	N(1)−C(7)−C(8)	119.6(9)
N(3)−C(13)−C(12)	116.9(6)	N(3)−C(25)−C(24)	118.6(6)	N(3)−C(13)−C(12)	117.6(8)
N(2)−C(8)−C(1)	116.7(6)	N(2)−C(20)−C(13)	117.4(5)	N(2)−C(8)−C(7)	117.6(8)
N(2)−C(12)−C(13)	116.5(6)	N(2)−C(24)−C(25)	116.9(5)	N(2)−C(12)−C(13)	118.7(8)
N(2)−C(8)−C(9)	122.0(6)	N(2)−C(20)−C(21)	122.7(6)	N(2)−C(8)−C(9)	121.5(9)
N(2)−C(12)−C(11)	121.8(7)	N(2)−C(24)−C(23)	122.4(6)	N(2)−C(12)−C(11)	121.8(8)
C(1)−N(1)−C(20)	121.3(6)	C(13)−N(1)−C(6)	120.7(5)	C(7)−N(1)−C(20)	118.7(8)
C(13)−N(3)−C(34)	122.0(6)	C(25)−N(3)−C(37)	120.2(5)	C(13)−N(3)−C(30)	119.0(8)
C(8)−N(2)−C(12)	119.2(6)	C(20)−N(2)−C(24)	117.7(5)	C(8)−N(2)−C(12)	117.7(7)
C(8)−C(9)−C(10)	119.0(7)	C(20)−C(21)−C(22)	118.5(6)	C(8)−C(9)−C(10)	120.3(9)
C(12)−C(11)−C(10)	118.6(7)	C(24)−C(23)−C(22)	119.7(6)	C(12)−C(11)−C(10)	118.0(9)
C(9)−C(10)−C(11)	119.2(6)	C(21)−C(22)−C(23)	118.9(6)	C(9)−C(10)−C(11)	120.6(9)

yields of 63% and 39%, respectively (Scheme 2). A clear indication of the steric demands of these two ligand systems was reflected in the NMR spectra of **2** and **3**. Specifically, the appearance of diastereotopic Me groups for **2** and diastereotopic CH_2 groups for **3** was consistent with hindered rotation of the N_{imine}−Ar′ bonds in these compounds. Complex **2** displayed two broad, equal intensity doublets for the ^{i}Pr methyl groups, and the uniqueness of these groups was confirmed by the appearance of two singlets for these methyl goups in the ^{13}C NMR spectrum of **2**. Attempts to carry out NMR experiments for the ethyl compound, **3**, in $CDCl_3$ were unsuccessful. These observations can be attributed to traces of HCl in the $CDCl_3$ or to oxidative addition reactions of the alkyl halide to the In (I) complex, which resulted in conversion of **3** to an In^{3+} species.[17]

The detailed structural features of **2** and **3** were established by single crystal X-ray analysis studies, which confirmed these species as the bis(imino)pyridine complexes [{2,6-$R_2C_6H_3N$=CPh}$_2$(NC_5H_3)]$In^+(OTf)^-$ (R = iPr, **2**; Et, **3**). Pictorial representations for the structures of **2** and **3** are presented in Figures 2 and 3 with a summary of bonding parameters presented in Tables 1 and 2. Notwithstanding the low data resolution for compound **3**, the structure obtained is consistent with noncrystallographic spectroscopic results and with independent theoretical computational optimization albeit the metric data must always be interpreted mindful of the larger statistically estimated experimental errors.

The general structural features for the cations in compounds **2** and **3** are evocative of those observed for **1**. In particular the In−N_{py} distances (**2** In1−N2 2.502(5) Å, **3** In1−N2 2.501(8) Å) are the same as was observed in **1**. Furthermore, the In−N_{imine} distances for **2** (In1−N1 2.664(5) Å, In1−N3 2.679(5) Å) and **3** (In1−N1 2.731(8) Å, In1−N3 2.637(6) Å) are greater than the sum of the covalent radii for these two elements. Again, like compound **1**, the imine C=N distances within **2** and **3** are comparable to those for the free ligand.

The reduction of the size of the aryl substituents in **2** and **3**, compared to **1**, allowed for a closer approach of the OTf^- anions to the In centers. For compound **2** the shortest In−O (In1−O1) distance was 2.462(6) Å while for compound **3** a slightly longer distance for In1−O1 of 2.532(7) Å was obtained. For comparison, these distances are shorter than those reported for In(OTf) (In−O 2.579(6) Å and 2.589(6) Å)[7] but considerably longer than in InOTF[18]crown-6 where the In−O distance was 2.370(2) Å.[6] The orientation of the triflate anions in compounds **2** and **3** suggests an alignment of the negative charge density of the O and F centers with $\delta+$ charges on the imino-carbon ligand sites (i.e., **2** C13, C25; **3** C7, C13). The specific differences in triflate anion orientation for **2** and **3**, as shown in Figures 2B and 3B, is likely an indication for a low energy barrier to reorganization of the anion.

(17) Hill, M. S.; Hitchcock, P. B.; Pongtavornpinyo, R. *Inorg. Chem.* **2007**, *46*, 3783.

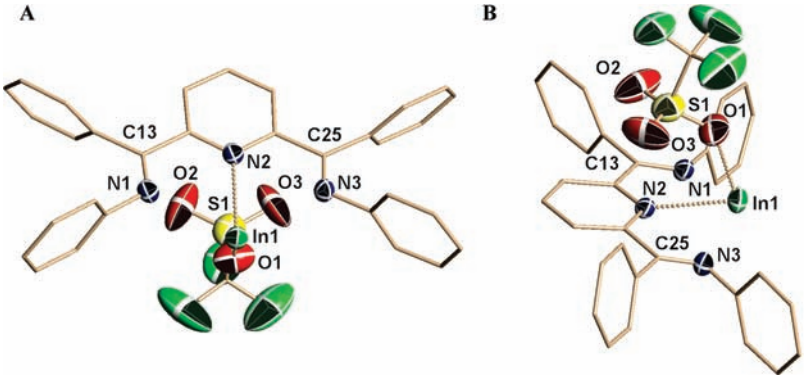

Figure 2. X-ray structure (A: top view, B: side view) of compound **2**, with hydrogen atoms and ^{i}Pr groups omitted for clarity. Selected bond lengths and angles are given in Tables 1 and 2, respectively.

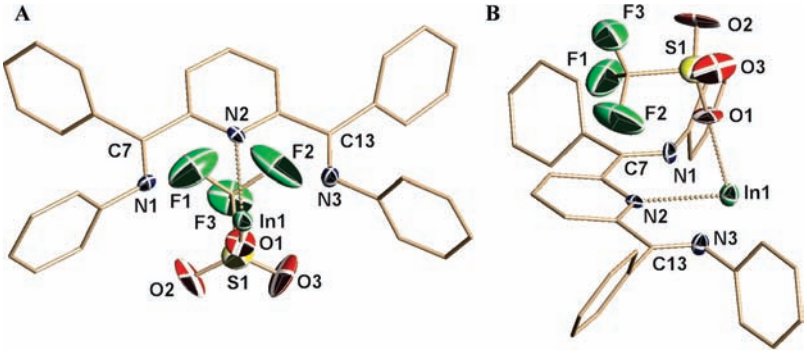

Figure 3. X-ray structure (A: top view, B: side view) of compound **3**, with hydrogen atoms and ethyl groups omitted for clarity. Selected bond lengths and angles are given in Tables 1 and 2, respectively.

Scheme 3

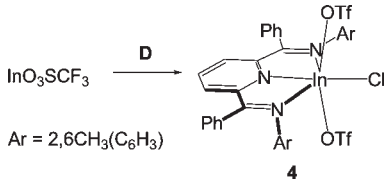

In striking contrast to the syntheses of the In (I) compounds **1**−**3**, ligand **D** reacted with $In(O_3SCF_3)$, to generate a red reaction mixture (Scheme 3). The only pure material isolated from this mixture was an In(III) bis(imino)pyridine complex, $[\{2,6\text{-}Me_2C_6H_3N{=}CPh\}_2(NC_5H_3)]In(OTf)_2Cl$ **4**, possessing two $^{-}O_3SCF_3$ anions and one chloride ion. Large yellow block-like crystals were isolated and subjected to elemental analysis confirming homogeneity of the crystallized product. When these reactions were repeated using different precursor batches, including samples with satisfactory carbon microanalysis, only compound **4** could be isolated from the reaction mixture. Variable quantities of indium metal powder were observed in these reactions, indicative of some disproportionation reaction. We attribute the appearance of the chloride ligand in compound **4** to a slight impurity arising from the synthesis of InOTf.

As shown in Figure 4, compound **4** displayed a distorted octahedral coordination geometry for In (III) with the coordination sphere consisting of a planar, tridentate bis(imino)-pyridine ligand $\{2,6\text{-}Me_2C_6H_3N{=}CPh\}_2(NC_5H_3)$ with the remaining three coordination sites occupied by two, *trans*-oriented triflate anions and a chloride anion. The distances for In−N (In1−N1 2.289(3) Å, In1−N2 2.171(4) Å) and

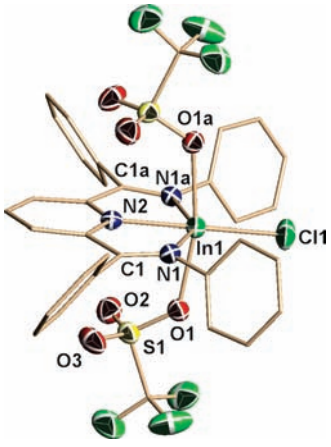

Figure 4. X-ray structure of compound **4**, with hydrogen atoms and methyl groups omitted for clarity. Selected bond lengths and angles are given in Table 3.

In−Cl (In1−Cl1 2.312(2) Å) in **4**, as well as the ligand features, are comparable with the metrical parameters for the recently reported cationic bis(imino)pyridine indium(III) complex $[\{2,5\text{-}^{t}Bu_2C_6H_3N{=}CPh\}_2(NC_5H_3)]InCl_2^{+}$ where average In−N and In−Cl distances of 2.27 Å and 2.33 Å, respectively, were observed.[2] The In1−O1 distance of 2.269(3) Å and the observed S−O bond distances of the triflate anion (S1−O1 1.476 Å, S1−O2 1.424 Å, S1−O3 1.431 Å) are consistent with coordination of O1.[7,18]

(18) Andrews, C. G.; Macdonald, C. L. B. *J. Organomet. Chem.* **2005**, *690*, 5090.

Table 3. Selected Bond Distances and Bond Angles for Compound and **4**

selected bond lengths (Å)		selected bond angles (deg)	
In(1)−N(1)	2.289(3)	In(1)−N(2)−C(2)	118.7(2)
In(1)−N(2)	2.171(4)	In(1)−N(1)−C(1)	115.2(2)
In(1)−O(1)	2.269(3)	N(1)−C(1)−C(2)	117.4(3)
In(1)−Cl(1)	2.312(2)	N(2)−C(2)−C(1)	114.8(3)
N(1)−C(1)	1.285(4)	N(2)−In(1)−N(1)	73.53(7)
N(2)−C(2)	1.340(4)	N(2)−In(1)−Cl(1)	180.00(1)
N(1)−C(11)	1.463(4)	N(2)−In(1)−O(1)	83.46(6)
S(1)−O(1)	1.476(3)		
S(1)−O(2)	1.425(3)		
S(1)−O(3)	1.431(3)		

Computational Evaluation

A DFT computational study with the B3LYP functional and the mixed DZVP/TZVP basis set was undertaken to obtain a thorough understanding of the electronic nature of the In[bis-(imino)pyridine]$^+$ cations and the interactions of the cation with the OTf$^-$ anion in compounds **1**−**3**. Optimizations for compounds **1**−**3** gave structures that were in agreement with the experimental structures. In the case of compound **1**, the analysis of the electronic structure of the cation pointed toward only nominal covalent interactions of the In cation with the ligand.[2] Specifically, the natural population analysis (NPA) for the valence configuration of the In(I) center was $5s^{1.93}5p^{0.20}$, and the NPA-derived charge of the In atom was +0.86 au. These results indicated that much of the cationic charge remains on the In, and only 0.14 electrons are transferred from the ligand to In$^+$ in the complex. Analysis for the cation component of **2** gave very similar results with a charge on the indium center of +0.83 au and only 0.17 electrons transferred from the ligand in this case. For comparison, the NPA-derived charge of the Ge(II) center in the complex (Ge cryptand[2.2.2])$^{2+}(O_3SCF_3)^-{}_2$, which displayed minimal coordination between the cryptand ligand and Ge, was +1.38 au and corresponded to 0.62 electrons being donated to the Ge(II) ion.[1] This is significantly stronger charge donation than obtained for **1** or **2**.

These results were convincingly supported by the bond order analysis. In the case of the cation of **1**, Mayer bond order values for In−N1/In−N3 and In−N2 interactions are only 0.23 and 0.28, respectively. Similarly, for the cation in **2**, the In−N_{imine} (In−N1/In−N3) interactions corresponded to a bond order of 0.19 while an In−N2 bond order of 0.22 was obtained. These values are all subtantially lower than the expected indices of 1 for single bonds. The Wiberg bond indices calculated in the natural atomic orbital basis are only 0.07−0.10, also consistent with very weak In-ligand interactions. These observations are also in harmony with the extremely long In−N distances in these species.

While the triflate anion of **1** was well beyond bonding distance, the shortest OTf$^-$ contact in **2** was at an In−O distance of 2.462(6) Å. A careful examination of the cation/anion pair alignment observed in both the crystallographic (Figure 3B) and the computational structures of **2** suggests a significant electrostatic component to the interaction energy for the ion pair. Specifically, the negatively charged oxygen atoms of triflate (the average NPA charge of O is −0.94 au) are positioned over the sites of positive charge localization of the cation: In, C_{imine} (C13, C25 = +0.30 au) and C_{py} (C20, C24 = +0.17 au). The results of energy decomposition analysis support that the major component of the interaction energy between the two ions ($E_{int} = -82.9$ kcal mol^{-1}) is, in fact, electrostatic with only approximately 40% of the cation/anion energy because of orbital interactions ($E_{orb} = -32.7$ kcal mol^{-1}).

The precise orbital contributions to the interaction energy were explored in more detail by examining the specifics of the electron transfer from the triflate anion to the In[bis(imino)-pyridine]$^+$ cation through a fragment orbital population analysis. Only 0.21 electrons are transferred from the anion to the cation and, of these, only 0.10 electrons are transferred to a cation fragment orbital that has a significantly In-based component. This lowest unoccupied fragment orbital (LUFO+2) is 85% In 5p in nature. This analysis provided further validation that the indium center in the cation receives only minor electron donation from the OTf$^-$ anion with the bulk of electron donation actually going to the ligand component of the In[bis(imino)pyridine]$^+$ cation. The donation from the triflate to indium corresponds to an In−OTf bond order of only 0.17.

An optimization for the In[bis(imino)pyridine]$^+$ cation in **2** was also carried out in the absence of the OTf$^-$ anion. The computed structure for this cation yielded In−N distances that are in agreement with the experimental In−N distances in **2** (In−N_{py}: 2.57 Å vs 2.502(5) Å exp and In−N_{imine}: 2.63 Å vs 2.66 Å exp). These results also point to electrostatic rather than orbital interaction for the association of the anion with the cation in **2**.

Computational methods provide a valuable approach to explore the role of substituents of the aryl group on N_{imine}−Ar′ sites of the In[bis(imino)pyridine]$^+$ cations. Consequently, a DFT optimization of the model cation [{C_6H_5N=CPh}$_2$(NC_5H_3)]In$^+$, with unsubstituted phenyl groups, was performed. This was an attempt to evaluate the role of both ligand sterics and of the counterion in our computational analysis of the cation. Interestingly, under these model conditions, the computed values for the In−N_{py} (2.52 Å) and the In−N_{imine} (2.63 Å) distances are essentially identical to the crystallographic values obtained for **1**−**3**. Significantly, this model system analysis again provided only nominal bonding between the bis-(imino)pyridine ligand and the In$^+$ center with bond orders for the In−N_{py} of 0.27 and for In−N_{imine} of 0.24.

For the more simplified In[bis(imino)pyridine]$^+$ cation with Ar′ = H, the bonding between the In$^+$ cation and the ligand was analyzed more intimately using a molecular orbital interaction diagram (Figure 5). Three occupied fragment orbitals (HOFO, HOFO-1 and HOFO-3) of the ligand participate in the charge donation to the two σ-type 5p orbitals (p_x and p_z) of the In$^+$ cation. The In p_y orbital is non-bonding with the ligand π-framework. There is no back-donation from the metal into the extended π-system since In 5s → L π*, is symmetry forbidden (zero overlap, see Figure 5). Only the ligand HOFO-3 mixes with the occupied In 5s orbital. For the In[bis(imino)-pyridine]$^+$ cations, the lone pair of electrons on In$^+$ is localized in the 5s orbital, and the raising of the energy of these electrons is a dominant feature in a destabilizing effect on the metal−ligand bonding (Figure 5). For the In[bis(imino)pyridine]$^+$ cation with Ar′ = H, the highest occupied molecular orbital (HOMO) of the cation has 74% contribution from In-localized orbitals (Figure 5, Table 4). Elaboration of the N_{imine}−Ar′ groups of the In[bis(imino)pyridine]$^+$ cations (Ar′ = Ph, 2,6-^{i}Pr$_2$C$_6$H$_3$, 2,5-^{t}Bu$_2$C$_6$H$_3$) significantly reduced the contribution from In-localized orbitals and, most importantly, of the lone electron pair in In 5s to the HOMO of the cation as summarized in Table 4. As a result the reactivity of the In(I) lone pair of electrons is diminished, and we propose that this effect plays a critical role in leading to the stable complexes **1**−**3**.

The decrease in In 5s contribution to the HOMO arises primarily from two effects. The first is because changing Ar′ from H to substituted phenyl groups increases the number of occupied electronic levels of the ligand which can mix with the 5s orbital, and this distributes the In orbital over a larger number of In[bis(imino)pyridine]$^+$ orbitals. The second contribution arises from the fact that as the ligand changes from Ar′ = H to ligands **A**−**C**, the energy of the occupied orbital of the bis(imino)pyridine fragment that overlaps with the In 5s (i.e., the analogue of the HOFO-3 in Figure 5) rises in energy. As a result, the mixing between In 5s and this ligand orbital

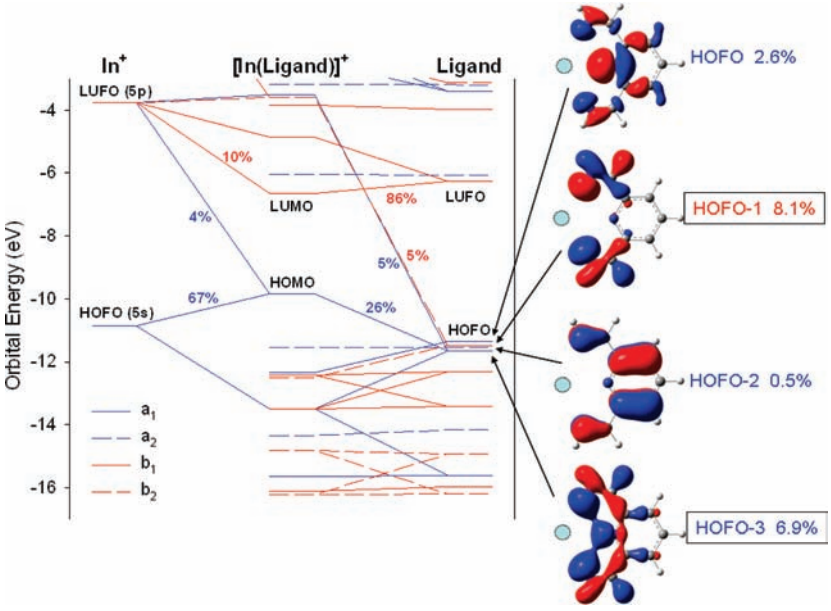

Figure 5. Molecular orbital interaction diagram for the di(imino)pyridine ligand (Ar′ = H) and the In^+ cation. The four highest occupied fragment orbitals (HOFOs) of the ligand and their contribution to the ligand-to-metal charge transfer interactions in the complex (via the % of electron population transferred to the In^+ cation) are shown on the right.

Table 4. Energy and % In Character in the HOMO of In[bis(imino)pyridine]$^+$ Cations

Ar′	ε_{HOMO} (eV)	% In (% In s)[a] character in HOMO
H	−9.84	74% (66%)
Ph	−8.82	57% (47%)
2,6-^{i}Pr$_2$C$_6$H$_3$	−8.52	37% (28%)
2,5-^{t}Bu$_2$C$_6$H$_3$	−8.56	19% (14%)

[a] Indium s orbital contribution (%).

leads to the HOMO that has a lower In character and higher contribution of ligand occupied orbitals.[19]

Conclusion

The sterically demanding bis(imino)pyridine scaffold readily reacted with the In(I) synthon, In(O_3SCF_3), to allow the preparation, isolation, and analysis of a set of exceptional compounds in which the In^+ cation is involved in only minimal covalent interactions with the ligand and counterion. The In^+ centers in these compounds are electron deficient possessing a 5s lone pair of electrons, and three unoccupied p orbitals. Structural features of the compounds point to weak coordination, and computational analysis of the two σ-type 5p orbitals revealed that they only receive limited electron donation from the ligands. While the reduction in the steric demands of the ligand did allow for closer approach of the triflate counterion to the In centers, the major component of the interaction energy between the two ions was determined to be electrostatic in nature with substantial component of the interaction to be between the ligand and the OTf^- anion. The indium center receives only minor electron donation from the anion.

In line with the observations that ligand sterics play an important role in stabilizing these species, by reducing the ligand steric demands to Ar′ = 2,6-$Me_2C_6H_3$ the In(III) bis(imino)pyridine complex, [{2,6-$Me_2C_6H_3N$=CPh}$_2$(NC_5H_3)]In($OTf)_2$Cl **4**, was produced. Electronic structure analysis demonstrated that only one ligand donor orbital mixes with the In 5s orbital and that this four electron interaction decreases as the steric demands of the imino-aryl groups increases, leading to the HOMO that is dominated by ligand contributions over the In lone pair.

In spite of having three N donor centers, the bis(imino)-pyridine ligand, while stabilizing a low valent metal center, provides little charge donation to the metal cation because of the "mismatch" of donor orbital of the ligand and the sp metal acceptor orbitals (Figure 5). Using this strategy, we are in the process of targeting other low-valent compounds.

Experimental Section

General Methods. Reactions were performed in a glovebox with a nitrogen atmosphere, with the exception of ligand synthesis, which was performed using standard Schlenk techniques under a flow of N_2. All solvents were sparged with nitrogen and then dried by passage through a column of activated alumina using an apparatus purchased from Anhydrous Engineering. Deuterated chloroform was dried using activated molecular sieves. Metal halides were purchased from Strem Chemicals and used as received. All other chemicals were purchased from Aldrich and used without further purification. Compounds **A**, **B**, and **1** were synthesized according to literature procedures.[2,20] ^{1}H and ^{13}C NMR spectra were run on a Bruker Avance 300 MHz spectrometer with $CDCl_3$, CD_2Cl_2, and DMSO-d_6 as solvents and internal standards. Elemental analyses for **A**−**D**, and **1**−**4** were performed by Midwest Microlab LLC, Indianapolis, IN.

2 6-Bis{1-[(2,6-diethylphenyl)imino]-benzyl}pyridine (C). Under a nitrogen atmosphere, a mixture of 2,6-dibenzoylpyridine (1.0 g, 3.48 mmol), a slight excess of 2,6-diethylaniline (1.143 g, 7.66 mmol), and *p*-toluenesulfonic acid (0.1 g) in toluene (150 mL) were placed in a round-bottom flask that was equipped with a Dean−Stark trap. The reaction mixture was heated to 160 °C, using a sand bath, for 48 h. The workup was performed under lab atmosphere conditions. The reaction mixture was allowed to cool to room temperature, and the solvent was removed under vacuum to give a dark yellow oil. Cold methanol was added to the oil, and the solution was held at

(19) Composition of the HOMO in terms of fragment orbitals is provided in the Supporting Information, Table S2.

(20) Jurca, T.; Dawson, K.; Mallov, I.; Burchell, T.; Yap, G. P. A.; Richeson, D. S. *Dalton Trans.* **2010**, *39*, 1266.

−20 °C for 48 h, over which time a multitude of large yellow rectangular crystals formed. The solid was removed by filtration, and the crystals were washed with cold methanol and hexanes. The crystals were then crushed to a fine pale yellow powder, and held under vacuum for 72 h to remove remaining methanol. A very fine pale yellow powder was collected in moderate 39% yield (750 mg, 1.36 mmol), but in high purity: Analysis for $C_{39}H_{39}N_3$ Calculated: C, 85.21; H, 7.15; N, 7.64 Found: C, 85.13; H, 7.17; N, 7.63. Room temperature ^{1}H NMR ($CDCl_3$, 300 MHz) and ^{13}C NMR NMR ($CDCl_3$, 75 MHz) showed a number of resonances which could not be definitively assigned and were attributed to a fluxional species. ^{1}H NMR (T = 115 °C, d_6-dimethyl sulfoxide, 300 MHz) δ 7.77(br t, 1 H, py, *p*-CH), 7.52−7.27 (br m, 12 H, py-CH, Ar−H), 6.93 (br m, 6H, Ar−H), 2.37(br s, 8H, CH_2), 1.07(t, 12H, CH_3). ^{13}C NMR (T= 115 °C, d_6-dimethyl sulfoxide, 75 MHz) δ 164.9 (C═N imine), 155.0-(py-C), 147.5(Ar−CH), 137.4(Ar−C), 136.8(Ar−CH), 131.0(Ar−CH), 130.3(Ar−C), 128.7(Ar−CH), 128.2(Ar−CH), 125.5(Ar−CH), 123.3(Ar−CH), 122.8(Ar−C), 24.4(−CH_2), 13.3(−CH_3).

2,6-Bis{1-[(2,6-dimethylphenyl)imino]-benzyl}pyridine (D). Following the procedure described for **C**, a mixture of 2,6-dibenzoylpyridine (1.0 g, 3.48 mmol), an excess of 2,6-dimethylaniline (1.10 g, 9.08 mmol), *p*-toluenesulfonic acid (0.1 g) in toluene (150 mL) were placed in a round-bottom flask under nitrogen atmosphere, and the reaction flask was equipped with a Dean−Stark trap. The reaction mixture was heated to 160 °C, using a sand bath, for 48 h. The workup was performed under lab atmosphere conditions. The reaction mixture was cooled to room temperature, and the solvent was removed under vacuum to give a dark yellow oil. Cold methanol was added to this oil, and the solution was held at −20 °C for 24 h, over which time a bright yellow precipitate formed. The precipitate was removed by filtration, and washed with cold methanol and hexanes to afford a fine yellow powder. The powder was further purified by flashing through a silica plug with 15:1 hexanes/ethyl acetate. The solvent was removed under the vacuum to afford a very fine yellow powder in moderate 47% yield (809 mg, 1.64 mmol), but in high purity. Analysis for $C_{35}H_{31}N_3$ Calculated: C, 85.16; H, 6.33; N, 8.51 Found: C, 85.30; H, 6.47; N, 8.41. Room temperature ^{1}H NMR ($CDCl_3$, 300 MHz) and ^{13}C NMR NMR ($CDCl_3$, 75 MHz) showed a number of resonances which could not be properly assigned and were attributed to a fluxional species. ^{1}H NMR (T=115 °C, d_6-dimethyl sulfoxide, 300 MHz) δ 8.20−7.65(br m, 3 H, py, CH), 7.39 (v br s, 10 H, Ar−H), 6.89 (br m, 6H, Ar−H), 1.99(m, 12H, CH_3). ^{13}C NMR (T=115 °C, d_6-dimethyl sulfoxide, 75 MHz) δ 165.7 (C═N imine), 155.2(py-C), 148.6(Ar−CH), 137.5(Ar−C), 136.9(Ar−CH), 130.3(Ar−C), 128.5(Ar−CH), 128.2(Ar−CH), 127.6(Ar−CH), 125.3(Ar−CH), 122.9(Ar−CH), 122.7(A-C), 18.1(−CH3).

[In-2,6-Bis{1-[(2,6-diisopropylphenyl)imino]-benzyl}pyridine]-[OSO_2CF_3] (2). $InOSO_2CF_3$ powder (87 mg, 0.331 mmol) was added to a clear yellow solution of **B** (200 mg, 0.331 mmol) in 5 mL of toluene. The reaction mixture was sealed and allowed to stir for 6 h. An immediate color change from translucent yellow to translucent red-orange was observed, with a gradual change to dark red. The solution was then held at −20 °C for 24 h, and a small amount of orange precipitate formed. This solution was filtered, and the precipitate was washed with 2 × 5 mL of hexanes, and allowed to dry under vacuum. An orange powder of **2** was isolated in 63% yield. Yellow-orange needle like crystals suitable for X-ray analysis were grown by diffusion of hexanes into a saturated tetrahydrofuran (THF) solution of **2** and storing at −20 °C for several days. ^{1}H NMR ($CDCl_3$, 23 °C): δ 7.99(t, 1H, py, *p*-CH), 7.68(d, 2H, py, *m*-CH), 7.46−7.28(br m, 10H, Ar−H), 7.16−7.02(br m, 6H, Ar−H) 3.00(br m, 4H, ^{i}Pr-CH), 1.20(br d, 12H, CH_3), 0.91(br d, 12H, CH_3). ^{13}C NMR ($CDCl_3$). δ 167.4(C═N imine), 154.6(py-C), 141.7(py-CH), 140.3(Ar−C), 138.7(py-CH), 133.7(Ar−CH), 130.6(Ar−C), 130.2(Ar−C), 129.6(Ar−CH), 128.7(Ar−CH), 126.3(Ar−CH), 123.8(Ar−CH), 28.6(CH_3), 26.3(*C*HMe$_2$), 22.7(CH_3). Analysis for $C_{44}H_{47}F_3InN_3O_3S$ Calculated: C, 60.76; H, 5.45; N, 4.83 Found: C, 60.61; H, 5.29; N, 4.82.

[In-2,6-Bis{1-[(2,6-diethylphenyl)imino]-benzyl}pyridine][OSO_2CF_3] (3). $InOSO_2CF_3$ powder (90 mg, 0.341 mmol) was added to a clear yellow solution of **C** (194 mg, 0.353 mmol) in 5 mL of hexanes. The reaction mixture was sealed and allowed to stir for 18 h. A gradual color change from translucent yellow to opaque orange was observed, as the $InOSO_2CF_3$ slowly went into solution. The solution was then held at −20 °C for 24 h, and a pale orange precipitate formed. This solution was filtered, and the precipitate was washed with 5 × 2 mL of hexanes, and allowed to dry under vacuum. The resulting pale orange powder was then dissolved in toluene, and then the solution was passed through a plug of Celite to remove impurities. The solution was then dried under vacuum, resulting in the isolation of a dark orange powder in a modest yield of 39% (108 mg) because of mechanical loss from purification. Dark orange rod-like crystals suitable for X-ray analysis were grown by diffusion of hexanes into a saturated toluene solution of **3** and storing at −20 °C for several days. ^{1}H NMR (C_7D_8, 23 °C): δ 7.45(v br s, 4H, Ar−H), 7.26(d, 2H, py, m-CH), 7.09(br s, 2H, Ar−CH), 7.02−6.82(br m, 11H, Ar−H), 2.79(br m, 4H, CH_2), 2.41(br m, 4H, CH_2), 1.20(t, 12H, CH_3). ^{13}C NMR (C_7D_8) δ 168.2 (C═N imine), 155.1(py-CH), 144.1(py-C), 140.5(py-CH), 134.9(Ar−CH), 134.1-(Ar−CH), 130.6(Ar−CH), 129.9(Ar−C), 129.7(Ar−CH), 129.6−128.7 (Ar−CH overlapped by C_7D_8 signals), 126.3(Ar−CH), 126.1-(Ar−C), 123.9(Ar−C), 25.5(CH_2), 15.4(CH_3). Analysis for $C_{40}H_{39}F_3InN_3O_3S$ Calculated: C, 59.05; H, 4.83; N, 5.16 Found: C, 58.87; H, 4.85; N, 4.98.

[In(OSO_2CF_3)$_2$Cl-2,6-Bis{1-[(2,6-dimethylphenyl)imino]-benzyl}pyridine] (4). $InOSO_2CF_3$ powder (52.5 mg, 0.199 mmol) was added to a clear yellow solution of **D** (100 mg, 0.203 mmol) in 5 mL of toluene. The reaction mixture was sealed and allowed to stir for 4 h. An immediate color change from translucent yellow to opaque dark red was observed. The solution was then held at −20 °C for 5 days, and a dark red precipitate formed. This solution was filtered, and the precipitate was washed with 5 × 2 mL hexanes, and allowed to dry under vacuum. A red/bronze powder was isolated in 103 mg. Attempted crystallization in a range of solvents from three separate reactions using different purified precursor batches consistently yielded the same decomposition product **4**. Large block-like crystals could be consistently isolated, and were subjected to elemental analysis, confirming a relative homogeneity of crystallized product. Analysis for $C_{37}H_{31}F_6InClN_3O_6S_2$ Calculated: C 47.17, H 3.32, N 4.46, Found C 46.15, H 3.60, N 4.22.

Structural Determination of Compounds 1−4. Single crystals were mounted on a thin glass fiber and held in place using viscous oil. They were subsequently cooled to data collection temperature. Crystal data and details of the measurements are summarized in the Supporting Information, Table S1. Data were collected on a Bruker AX SMART 1k CCD diffractometer using 0.3 ω-scans at 0, 90, 180 in Φ. Unit-cell parameters were determined from 60 data frames collected at different sections of the Ewald sphere. Semiempirical corrections based on equivalent reflections were applied (Blessing, R., *Acta Crystallogr.* **1995**, *A51*, 33−38). The structures were solved and refined using the SHELXTL program suite (Sheldrick, G. M. AXS, Madison, WI, 1997). Direct methods yielded all non-hydrogen atoms which were refined with anisotropic thermal parameters. All hydrogen atom positions were calculated geometrically and were riding on their respective carbon atoms. Despite repeated attempts, compound **3** consistently yielded highly mosaic crystals that diffracted weakly. The results presented correspond to the best of several trials. No diffraction was observed at 2θ greater than 44.3°, and the data set was truncated accordingly to support a reasonable signal-to-noise ratio.

Acknowledgment. We thank NSERC for funding.

Supporting Information Available: Crystallographic data (cif files) for compounds **2**−**4**. Details of computational methods. This material is available free of charge via the Internet at http://pubs.acs.org.